

Synthesis, Molecular Docking, Characterization, and Preliminary Evaluation of Some New 1, 3-Diazetid-2-One Derivatives as Anticancer Agents

Farah Haidar Abdulredha*, Monther Faisal Mahdi*, Ayad Kareem Khan*

*Department of Pharmaceutical Chemistry, College of Pharmacy, Mustansiriyah University, Baghdad, Iraq.

Article Info:

Received May 2023

Revised June 2023

Accepted June 2023

Corresponding Author email:

ph.farah.haidar@uomustansiriyah.edu.iq

orcid: <https://orcid.org/0000-0002-9866-8441>

DOI : <https://doi.org/10.32947/ajps.v24i1.1026>

Abstract:

A series of novel 1,3-diazetid-2-one derivatives were designed, synthesized, and evaluated preliminary (*In Vitro*) for their cytotoxic activity against the lung (A549) cancer cell line. GOLD software (version 2021.2.0) was used to conduct a molecular docking study;

the tested derivatives demonstrated significant anticancer activity compared to the reference drug (erlotinib). PLP-fitness values for the final compounds are 79.81, 80.80, and 81.57, respectively, whereas the reference ligand, erlotinib, had a value of 76.20. The synthesized compounds were identified and characterized using physicochemical parameters (melting points and R_f values), FTIR, $^1\text{H-NMR}$, and $^{13}\text{C-NMR}$ spectroscopy. According to the IC50 values for the synthesized derivatives, compounds N4a and N4b exhibit outstanding anti-proliferative activity with IC50 value of (7.51, 7.68) μM against A549 cell line, compared to erlotinib, which has an IC50 value of (11.5) μM .

Key words: 1,3-diazetid-2-one, Docking Study, Lung Cancer.

تخليق، دراسة النمذجة الجزيئية، تشخيص والتقييم المختبري لبعض مشتقات 1،3-ديازتدين-2-اون الجديدة كعوامل مضادة للسرطان

فرح حيدر عبد الرضا*، منذر فيصل مهدي*، أياد كريم خان*
*فرع الكيمياء الصيدلانية/ كلية الصيدلة/ الجامعة المستنصرية

الخلاصة:

سلسلة من مشتقات جديدة 1،3-ديازتدين-2-اون تم تصميمها وتصنيعها وتقييمها بشكل أساسي (في المختبر) لنشاطها السام للخلايا ضد خط الخلايا السرطانية في الرئة A549. تم استخدام برنامج GOLD الإصدار (2021.2.0) لإجراء دراسة الارساء الجزيئي، أظهرت المشتقات المختبرة نشاطاً كبيراً مضاداً للسرطان مقارنة بالدواء المرجعي (erlotinib). تراوحت قيم PLPfitness للمركبات النهائية من 79.81، 80.80 و 81.57 بينما كانت قيمة الدواء المرجعي (erlotinib) 76.20.

باستخدام المعلمات الفيزيائية والكيميائية (نقاط الانصهار وقيم معامل الأعاقلة)، باستخدام طيف الاشعة تحت الحمراء الدقيق، الرنين النووي البروتوني، والرنين النووي الكربوني، تم تشخيص وتوصيف المركبات المصنعة. أظهرت قيم IC50 للمركبات المحضرة أن المركبين N4a و N4b يظهران نشاطاً بارزاً مضاداً للتكاثر بقيمة IC50 تبلغ (7.51، 7.68) ميكرومولار مقابل خط خلية A549، مقارنةً بمركب erlotinib الذي تبلغ قيمته IC50 (11.5) ميكرومولار.



الكلمات المفتاحية: 1، 3-ديازيتدين -2-اون، دراسة الأرساء الجزيئي، سرطان الرئة.

Introduction

Cancer is an advancing disease and is the leading cause of death worldwide.^[1] Malignant tumors result from various temporal and spatial alterations in the physiology of cancerous cells. The primary hallmark of the illness is abnormal cell proliferation or neoplasia^[2]. Tumor cells' invasion of adjacent tissues and distant organs is the leading cause of morbidity and mortality in most cancer patients. Finding molecular differences between cancerous and healthy cells has been the primary objective of cancer research. Due to a greater understanding of molecular and tumor biology, cancer treatment paradigms have shifted significantly over the past fifteen years^[3]. Previously, only organs of origin or essential histomorphologic characteristics were used to diagnose and treat cancer. Surgery, radiation therapy, Chemotherapy, combination therapy, and laser therapy are common cancer treatments; however, Chemotherapy is a promising treatment option for cancer^[4]. 90% of chemotherapy failures are due to drug resistance during cancer invasion and metastasis.^[5] Numerous anticancer drugs directly damage cancer cells' DNA, which has the drawbacks of being non-specific and having a high level of toxicity^[6]. Target medicine has become a favored technique for accessing tumors while avoiding interstitial damage to healthy tissue^[7]. The epidermal growth factor receptor (EGFR) is a cell-surface tyrosine kinase belonging to the ErbB family^[8]. EGFR was the first cell-surface receptor to be recognized as an oncogene. Over thirty percent of breast malignancies, sixty percent of non-small-cell lung cancers, and forty percent of glioblastomas either overexpress or include activating mutations in EGFR family members^[9]. Erlotinib is a potent and

selective inhibitor of the tyrosine kinase of the human epidermal growth factor receptor (EGFR), which has been approved by the FDA for the treatment of NSCLC,

pancreatic cancer, polycythemia vera (PV) and other myeloproliferative disorders^[10].

Heterocyclic compounds are a family of molecules that serve a crucial role in health care and the development of prescription drugs^[11]. As a result, heterocyclic structures have played a vital role in anti-cancer treatment, appearing in a variety of available anti-cancer medicines^[12]. Nearly sixty percent of FDA-approved small-molecule drugs are nitrogen-containing heterocycles, with four-membered rings being particularly desirable scaffolds due to their structural rigidity and ability to assume a distinct three-dimensional (3D) structure^[13].

Materials and Methods

The FTIR spectrum was taken on a Tensor 27 Bruker (USA), Melting point was measured by glass capillary tube on Stuart melting point apparatus (UK), The proton NMR (499.67 MHz) and carbon NMR (125.66 MHz) spectra were determined by Bruker (USA) utilizing DMSO as solvent. (+)-(s)-Naproxen 99% and different aryl aldehydes from Hyperchem company (China), SOCl₂ from Thomas Baker (India), Phenyl Isocyanate from Sigma-Aldrich (Germany).

Synthesis of methyl (S)-2-(6-methoxynaphthalen-2-yl) propanoate [N1].

Naproxen (4.3 mmol) was dissolved in 15 ml dry methanol and chilled to (0 to -5)^oC. 0.32 mL (4.5 mmol) of thionyl chloride was added dropwise to the solution. The solution was then brought to room temperature, kept in a water bath at 40^oC



for 3 hours, and refluxed at 65°C. The mixtures were allowed to settle and evaporate at room temperature. The resulting mixture was diluted with 25 mL of cold water, filtered, and washed twice with a 10% w/v NaHCO₃ solution (2 x 10 mL). This resulted in the formation of white crystals of [N1]. The product was purified by recrystallization from absolute ethanol. TLC plates coated with silica gel were used to track the reaction's development.^[14]

White crystal, yield= 100%, m.p.= 88-89°C^[14], R_f value = 0.75 (Ethyl acetate/n-hexane/methanol 3:2:1). **FT-IR (cm⁻¹):** 1736 (C=O ester). **¹H-NMR:** δ 1.50 (d, 3H, CH₃), δ 3.39 (q, 1H, CH), δ 3.88 (s, 3H, ether OCH₃), δ 3.95 (s, 3H, ester OCH₃), δ 7.16-7.80 (m, 6H, Ar H). **¹³CNMR:** δ 13.95, δ 20.52, δ 52.19, δ (110.72-148.93) signals of aromatic carbon of rings, δ 168.71.

Synthesis of (S)-2-(6-methoxynaphthalen-2-yl) propane hydrazide [N2].

Compound [N2] was synthesized by dissolving (0.244g, 1mmole) of compound [N1] in 15 mL of absolute ethanol. The solution received an excess amount of hydrazine hydrate 99% (0.25 mL, 5 mmol). The mixture was refluxed for 8 hours. The solution was allowed to cool, and then ice-distilled water was added to precipitate the mixture. Then, to acquire pure products, the product was purified by recrystallization from absolute ethanol. TLC plates coated with silica gel were used to track the reaction's development^[15].

Off-white fluffy powder, yield= 80%, m.p.= 136-138 °C^[16], R_f value = 0.5 (Acetone/petroleum ether 1:1). **FT-IR (cm⁻¹):** 3303-3278 (NH₂), 3205 (N-H), 1633 (C=O of amide). **¹H-NMR:** δ 1.45 (d, 3H, CH₃), δ 3.69 (q, 1H, CH), δ 3.88 (q, 3H, OCH₃), δ 4.27 (brs, 2H, NH₂), δ 7.15-7.79 (m, 6H, Ar H), δ 9.30 (brs, 1H, NH). **¹³CNMR:** δ 18.66, δ 43.58, δ 55.42, δ

(105.95-157.30) signals of aromatic carbon of rings, δ 173.27.

General procedure for the synthesis of Schiff's bases compounds [N3a-c].

To synthesize compounds [N3a-c], a solution of suitable aromatic aldehydes (1mmole) in 10 mL of absolute ethanol was stirred with 2-3 drops of glacial acetic acid at room temperature for 30 minutes. Then add (0.244g, 1mmo) of compound [N2], to 15 mL of absolute ethanol and add to the first mixture, followed by stirring at room temperature for 30 minutes and refluxing at 70°C for 3 hours. The mixtures of compounds [N3a-e] precipitated in a round bottom flask, and the resulting precipitate was isolated via filtration, rinsed with cold water, and recrystallized from absolute ethanol. The progress of the reaction was monitored by silica gel-coated TLC plates.^[17]

(S)-2-(6-methoxynaphthalen-2-yl)-N'-(pyridin-4-ylmethylene) propanehydrazide (N3a)

Off-white fine powder yield= 81%, m.p.= 194-195°C, R_f value = 0.62 (Ethyl acetate/n-hexane 1:1). **FT-IR (cm⁻¹):** 3186 (N-H), 1671 (C=O amide), 1657 (C=N of pyridine ring), 1644 (C=N of imine). **¹H-NMR:** δ 1.50 (d, 3H, CH₃), 3.42 (q, 1H,CH), δ 3.85 (s, 3H, OCH₃), δ 7.11-8.83 (m, 10H, ArH), δ 8.60 imine H (s, 1H, CH), δ 11.49 (brs, 1H, NH). **¹³CNMR:** δ 18.49, δ 44.47, δ 55.60, δ (106.16-157.49) signals of aromatic carbon of rings, δ 148.77, δ 175.67.

(S)-N'-(furan-2-ylmethylene)-2-(6-methoxynaphthalen-2-yl) propane hydrazide (N3b).

Off-white fine powder yield= 79%, m.p.= 171-172°C R_f value = 0.875(Ethyl acetate/n-hexane 1:1). **FT-IR (cm⁻¹):** 3204 (N-H), 1664 (C=O of amide), 1643 (C=N of imine), 1203 and 1015 (C-O-C furan). **¹H-NMR:** δ 1.50 (d, 3H, CH₃), δ 3.79 (q, 1H, CH), δ 3.87 (s, 3H, OCH₃), δ 6.61-



7.87 (m, 9H, ArH), δ 8.12 imine H (s, 1H, CH), 11.30 (brs, 1H, NH). ¹³CNMR: 18.63, 44.49, 55.61, (106.09-157.58) signals of aromatic carbon of rings, 145.30, 175.34.

(S)-2-(6-methoxynaphthalen-2-yl)-N'-(2-nitrobenzylidene) propane hydrazide (N3c).

White powder yield= 83 %, m.p= 191-192°C R_f value = 0.75(Ethyl acetate/n-hexane/methanol 3:2:1) . **FT-IR (cm⁻¹):** 3189 (N-H), 1667 (C=O of amide), 1648 (C=N of imine), 1564 and 1370 (NO₂). **¹H-NMR:** δ 1.48 (d, 3H, CH₃), δ 3.40 (q, 1H, CH), δ 3.85 (s, 3H, OCH₃), δ 7.07-8.24 (M, 10H, ArH), δ 8.49 imine H (s, 1H, CH), δ 11.32 (s, 1H, NH). ¹³CNMR: δ 19.00, δ 44.53, δ 55.60, δ (106.14-157.57) signals of aromatic carbon of rings, δ 142.43, δ 175.41.

General procedure for the synthesis of 1,3-diazetidine-2-one derivatives [N4a-c].

The synthesis of (N4a-c) was carried out in a 100 ml round bottom flask. 1 mmole of (N3a-c) was dissolved in anhydrous 1,4-dioxane (25 mL), followed by the slow addition of phenyl isocyanate (1.5 mmole) dropwise at a temperature of 0- -5°C. The resulting mixtures were stirred for three hours at room temperature and refluxed for (5-7) hours. After evaporating the solvent at room temperature, the resulting solids were washed with a mixture of ethyl acetate: petroleum ether (1:1), filtered and dried. Recrystallization from absolute ethanol.^[13]

(2S)-2-(6-methoxynaphthalen-2-yl)-N-(2-oxo-3-phenyl-4-(pyridin-4-yl)-1,3-diazetidin-1-yl) propanamide (N4a).

Off-white powder yield= 60%, m.p= 168-169°C. **FTIR (cm⁻¹):** 3235 and 3282 (N-H), 3190 (C-H of diazetidine ring), 1743 (C=O of diazetidine ring), 1647 (C=O of amide overlapping with C=N of pyridine). **¹H-NMR:** δ 1.49 (d, 3H, CH₃), δ 3.57 (q,

1H, CH), δ 3.86 (s, 3H, OCH₃), δ 6.95 (s, 1H, diazetidine CH), δ 7.00-8.81 (m, 15H, ArH), δ 11.48 (brs, 1H, NH). ¹³CNMR: δ 18.9, δ 44.42, δ 55.59, δ 66.81, δ (106.11-157.57) signals of aromatic carbon of rings, δ 150.75, δ 153.01, δ 170.52.

(2S)-N-(2-(furan-2-yl)-4-oxo-3-phenyl-1,3-diazetidin-1-yl)-2-(6-methoxynaphthalen-2-yl) propanamide (N4b).

Off-white powder yield= 60%, m.p= 178-179°C. **FTIR (cm⁻¹):** 3325 and 3282 (N-H), 3140 (C-H of diazetidine ring), 1729 (C=O of diazetidine ring), 1647 (C=O of amide), 1207 and 1029 (C-O-C of ether overlapping with (C-O-C) of furan). **¹H-NMR:** δ 1.48 (d, 3H, CH₃), δ 3.57 (q, 1H, CH), δ 3.86 (s, 3H, OCH₃), δ 6.99 (s, 1H, diazetidine CH), δ 6.59-7.85 (m, 14H, ArH), δ 11.28 (brs, 1H, NH). ¹³CNMR: δ 18.62, δ 44.48, δ 55.60, δ 66.82, δ (106.09-157.57) signals of aromatic carbon of rings, δ 153.01, δ 170.27.

(2S)-2-(6-methoxynaphthalen-2-yl)-N-(2-(2-nitrophenyl)-4-oxo-3-phenyl-1,3-diazetidin-1-yl) propanamide (N4c).

Off-white powder yield= 73%, m.p= 181-182.5°C. **FTIR (cm⁻¹):** 3325 and 3271 (NH), 3186 (C-H of diazetidine ring), 1728 (C=O of diazetidine ring), 1650 (C=O of amide), 1562 and 1342 (NO₂). **¹H-NMR:** δ 1.47 (d, 3H, CH₃), δ 3.52 (q, 1H, CH), δ 3.86 (s, 3H, OCH₃), 6.95 (s, 1H, diazetidine CH), δ 7.06-8.20 (m, 15H, ArH), δ 11.29 (brs, 1H, NH). ¹³CNMR: δ 18.98, δ 44.50, δ 56.18, δ 66.82, δ (106.11-157.55) signals of aromatic carbon of rings, δ 153.01, δ 170.18. The procedure of the synthesis of the compounds was shown in Scheme (1).

Computational Methods

To predict the binding configuration of novel 1,3-diazetidin-2-one derivatives to EGFR, docking techniques were performed using GOLD Suite (v. 2021.2.0), a fully licensed CCDC tool.



Using CCDC Hermes Visualizer software (version 2021.2.0), protein, ligand, hydrogen bond interaction, short contact and bond length calculations were performed.

The Swiss ADME tool converts Chem Sketch's ligands into SMILE names. It also predicts the physicochemical properties and pharmacokinetic stats of a molecule's atoms. This is how BOILED EGG calculates the lipophilicity and polarity of molecules.

Replacing water molecules in the enzyme PDB protein EGFR with hydrogen atoms produces ionized versions and tautomeric forms of its amino acid constituents. CheBio3D (version 16.0) utilized the MM2 force field.

By applying the default values for all parameters, the CHEMPLP fitness function is used to evaluate each candidate solution. Then, distance- and angle-dependent hydrogens are accounted for when calculating steric complementarity between proteins and their ligands. After this, the candidate solutions are evaluated according to the piecewise linear potential function. This process produces each candidate's binding mode, docking pose, and binding energy, which are used to evaluate the interaction between EGFR's amino acid residues and the molecules we created.

In vitro cytotoxicity

Cell Culture

The Human Lung Cancer Cell Line (A549) was initially acquired from ATCC. This cell line was stored in the Cell Bank of the Tissue Culture Research Center at Al-Mustansiriyah University, specifically within the College of Pharmacy.

Storage and Resuscitation of Cell Line.

The cells were cryopreserved under liquid nitrogen (-80°C) for 24 hours. Upon thawing at 37°C, 10 milliliters of fresh medium were added, and the cells were

extracted by centrifugation. Subsequently, the cells were resuspended in 25 mL of fresh media and transferred to a 75 cm² flask for cultivation.^[18]

Cell Maintenance.

Complete media consisting of 50 mL of 10% FBS, 5 mL of 1% L-Glutamine, and 5 mL of Penicillin-Streptomycin-Amphotericin B100X were added to 500 mL of RPMI-1640 Medium used for cultivating A549. The cells were cultured in 75 cm² flasks in 95% humidified air at 37°C with 5% CO₂. The cells were washed with 5 mL of sterile PBS after they reached 90% confluence and then incubated in trypsin solution at 37°C for 2 minutes to release them from the flask bottom during a sterile passage. After transferring the cell suspension to a 50 mL conical tube, complete growth media was added to bring the volume up to 50 mL. After spinning the cells for 3 minutes at 1200 rpm, the resulting supernatant was thrown away.^[19]

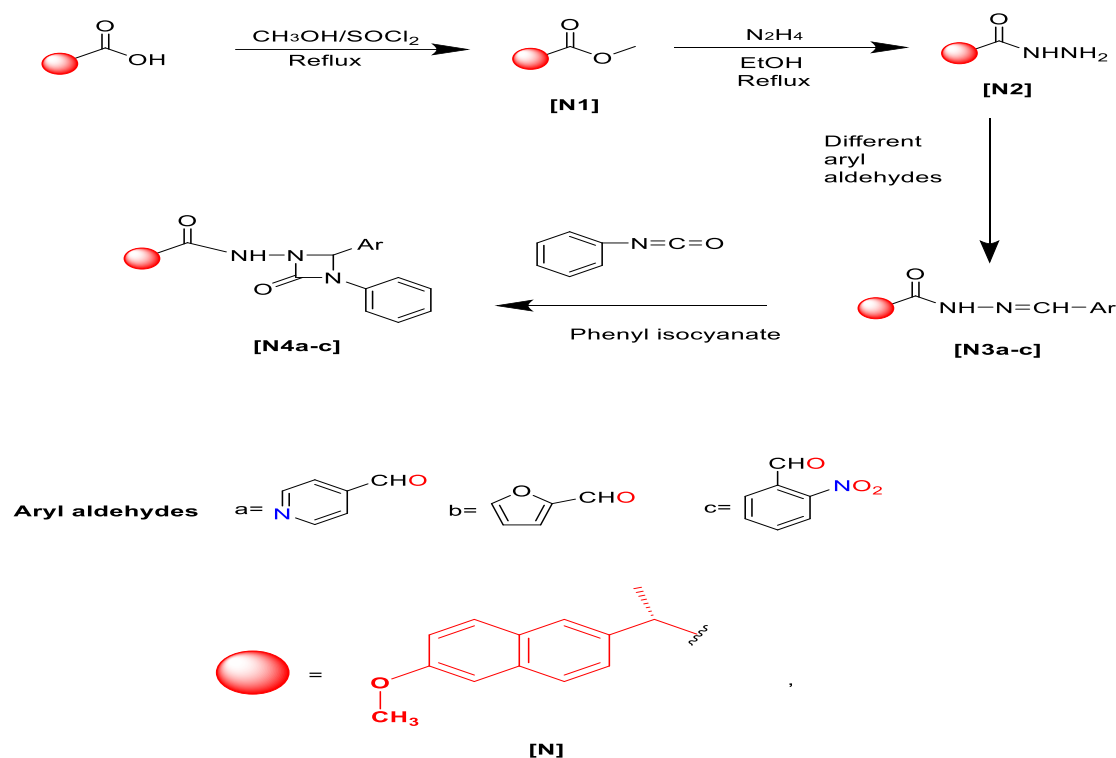
Cell Viability by MTT Colorimetric Assay.

The purpose of this investigation was to determine the impact of synthetic chemicals [N4a-c] on the viability of lung cancer cell lines using the MTT colorimetric assay. A cell suspension (100 µl) was placed at a concentration of (5 x 10³) cells per well in each well of a 96-well flat-bottom tissue culture plate, which was then incubated for 24, 48, and 72 hours. Each drug was added to the cells at a concentration of 5 M after 24 hours. After the recuperation periods (24hr, 48hr, and 72hr) were over, the cell culture medium was discarded, and the cultures were incubated at 37 degrees Celsius for 2 hours with a medium containing 10 l of MTT solution (5mg/ml MTT powder in PBS). After 2 hours, the medium was discarded, and 100 l of DMSO was added to each well, followed by 15-20 minutes of incubation in the dark at room temperature.



The transmission wavelength (560-600 nm) was used to measure the optical density of each plate (well) using a Multiscan Reader. Using the following formula, the rate of cell growth inhibition (% cytotoxicity) was calculated.

[Inhibition Rate percentage = (A-B/A) *100] where [A and B] are, respectively, the optical densities of the standard (erlotinib) and tested substances. The test was conducted in duplicate.^[20]



Scheme (1): The procedure of the synthesis of the compounds.

Determination of the Half-Maximal Inhibitory Concentration (IC₅₀).

Using a dose-response curve, it is possible to calculate the IC₅₀ of the tested compounds. About the in vitro MTT assay, the IC₅₀ is the concentration of the tested chemicals [N4a-c] necessary to reduce cell viability by 50%. Using the obtained results from the in vitro MTT experiment, the IC₅₀ values for the investigated drugs were computed 72 hours after their exposure to the cells. The concentration

range of substances [N4a-c] utilized to calculate IC₅₀ values was (500, 250, 125, 12.5, 62.5, 31.25, 15.62, 7.81, 3.90, and 1.95 μM).

Results and Discussion

Interpretation of synthesis results

The structure of compounds (N1) was identified by melting point and R_f value, FT-IR analysis, demonstrated that the broad peak of hydroxyl group of naproxen, at 2500-3200 cm⁻¹ disappeared. A signal at

(1736 cm^{-1}) for compound (N1), showed the existence of a carbonyl group of ester (-C=O), instead of the (C=O) of the carboxylic acid at (1724 cm^{-1}) for naproxen, (1228 cm^{-1}) for compound (N1) $\nu\text{C-O-C}$ stretching of ester. $^1\text{H-NMR}$ results have shown singlets of (-OCH_3) of ester at (3.95 (δ , ppm) for (N1), and the disappearance of broad peak of hydroxyl group at 12.39 (δ , ppm) for naproxen. $^{13}\text{C-NMR}$ showed peak for the carbonyl of the ester at (174.99) (δ , ppm) for (N1), while the methyl group showed a peak at 52.34 (δ , ppm). Infrared analysis (FT-IR) of compounds (N2), displays the disappearance of broadband at (1736 cm^{-1}) assigned to the carbonyl group (C=O) stretching of the ester of (N1), and the appearance of a new band at (1633 cm^{-1}) assigned to amide carbonyl group (C=O) stretching, as well as the (3303, 3278, and 3205 cm^{-1}) which are assigned to (-NHNH_2) group of (N2). $^1\text{H-NMR}$ spectra showed broad singlet for NH_2 protons of hydrazide at 4.27 (δ , ppm), and singlet for NH proton of hydrazide at 9.30 (δ , ppm) for (N2). $^{13}\text{C-NMR}$ showed the disappearance of the methyl ester peaks while revealing the carbonyl of the amide at (173.27) (δ , ppm).

FT-IR characteristic absorption bands of (N3a-c) shows νNH stretching of amide at (3204-3186 cm^{-1}), and combination band of $\nu\text{C=O}$ stretching of amide and $\nu\text{C=N}$ stretching at (1671-1664 cm^{-1}). $^1\text{H-NMR}$ spectra of compounds (N3a-c) showed singlet for N=CH-Ar (imine proton) at (8.12-8.60) (δ , ppm), and disappearance of the broad singlet for NH_2 protons of hydrazide. $^{13}\text{C-NMR}$ showed the peak of (-CH) imine at (\sim 142-145) (δ , ppm).

the FT-IR characteristic absorption bands of (N4a-c) showed N-H stretching vibration of secondary amide at (3235, 3271 cm^{-1}), giving two peaks because of hydrogen bond, In the presence of hydrogen bonding, the N-H stretch is split into two peaks: a lower frequency peak

and a higher frequency peak, the lower frequency peak corresponds to the N-H stretch in the hydrogen-bonded NH group, while the higher frequency peak corresponds to the N-H stretch in the non-hydrogen bonded NH group. Also, $\nu\text{C=O}$ stretching of diazetidine ring at (1743, 1728 cm^{-1}), $\nu\text{C=O}$ stretching of amide at (1650, 1647 cm^{-1}), -CH stretching of diazetidine ring at (3190, 3140 cm^{-1}). $^1\text{H-NMR}$ results have illustrated that the characteristic singlet peak for the imine proton has disappeared while showing a singlet peak at (6.95-6.99) (δ , ppm) of (-CH) proton of cyclic urea. $^{13}\text{C-NMR}$ have illustrated the characteristic singlet peak for the imine carbon has disappeared while showing the peak of (-CH) of the diazetidine ring at (61.86-66.82) (δ , ppm) and carbonyl of diazetidine ring at (153.01) (δ , ppm) (N4a-c).

Interpretation of docking results

The results of the docking study are the prediction of the best molecular interaction between the anticipated compounds (N4a-c) and the active binding sites of the EGFR proteins. The inhibitory activities were ranked by using the PLP fitness scores. Because it binds to the amino acids (AAs) residues of the active site via H-bonds and other short contacts, docking studies suggest that all of the anticipated compounds have excellent binding energies with receptor active pockets and are likely to have promising activity with EGFR proteins^[21]. The referenced ligand used to evaluate the binding, inhibition, and novel compounds were compared to erlotinib. All of the anticipated final compounds, exhibited higher binding energies, (79.81, 80.80, and 81.57) for (N4a-c), respectively, than the standard drug erlotinib, which gave PLP fitness value of (76.20). Docking analysis showed that VAL 702, LYS 721, THR830, LEU820, MET769, LEU768, GLY772, THR766, LEU764, and PHE832, for this



receptor and interact via hydrogen bonding and transient contacts with the proposed final ligand. Gold determines short contact and hydrogen bond distances between a protein atom and a proposed ligand.

Interpretation of ADME results

Drug similarity, or the degree to which a new substance is similar to an existing drug, is a crucial qualitative concept in the drug design process. This is determined from a compound's molecular structure prior to synthesis and testing, while "lead likeness" is defined as a compound's similarity to the structural and physicochemical properties of a "lead" compound..^[22]

All the predicted compounds had a bioavailability of 0.55 and TPSA of less than 140 Å², indicating that they all entered the systemic circulation. N4a and N4b pass the blood–brain barrier (BBB), whereas the N4c does not. (N4a and N4b) had an affinity for P-gp, the protein responsible for preventing chemotherapeutic agents from being internalized by cells, while N4c does not. As these compounds are P-gp substrates, efflux transporters will expel them from the cells^[23]. In addition, all predicted compounds complied with the Lipinski rule of five. ADME results were illustrated in table (1)

Table (1) Output parameters of drug-likeness and ADME.

Molecule No.	Compound name	n-HBA	n-HBD	TPSA (Å ²)	MR (m ³ /mol)	GI absorption	BBB permeability	Bioavailability score	Lipinski violation	Pgp
1	N4a	4	1	74.77	137.06	High	Yes	0.55	0	Yes
2	N4b	4	1	75.02	131.53	High	Yes	0.55	0	Yes
3	N4c	5	1	107.7	148.09	High	No	0.55	0	No

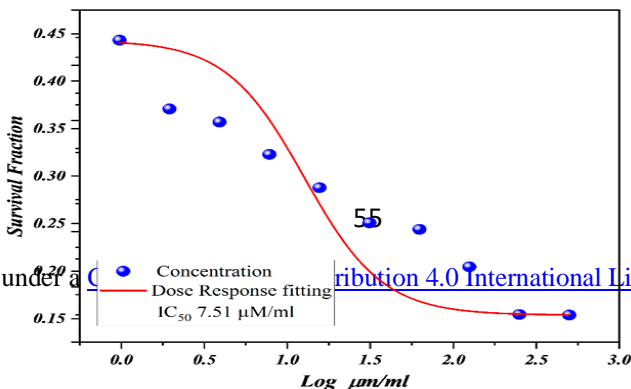
Interpretation of Cytotoxicity Results

All synthesized compounds exhibit outstanding anti-proliferative activity, with the exception of compound (N4c) compared with erlotinib at 72 hours. The IC₅₀ values of compounds N4a and N4b (7.51, 7.68) µM against A549 cell line, relative to erlotinib, which has an IC₅₀ value of (11.5) µM, while compound N4c IC₅₀ value was 12.77 µM which is slightly

higher than erlotinib IC₅₀. The dose-response curve of the synthesized compounds at 72 hours shown in figures (1, 2 and 3) for N4a-c, respectively. Also, morphological alterations of A549 cells following exposure to 62.5 µM of the synthesized compounds (N4a-c) at 48 hours were shown under the microscope when compared to A549 cells (control cell) in Figure (4, a, b, c, and d)

AJPS (2024)

AJPS is licensed under a



tribution 4.0 International License



Figure (1): Dose-response curve of IC₅₀ for compound N4a at 72 hours.

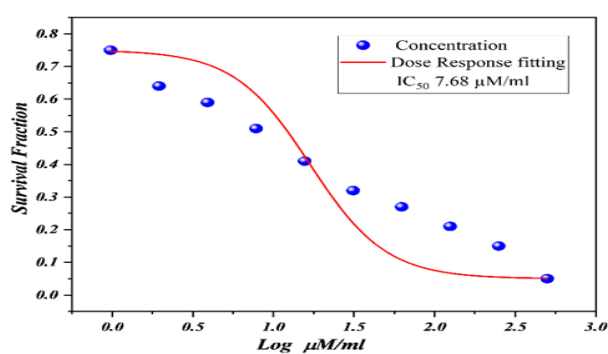


Figure (2): Dose-response curve of IC₅₀ for compound N4b at 72 hours.

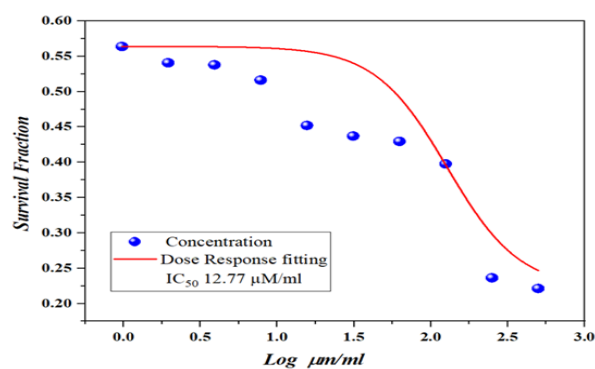
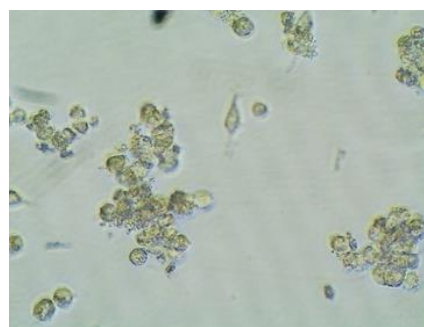
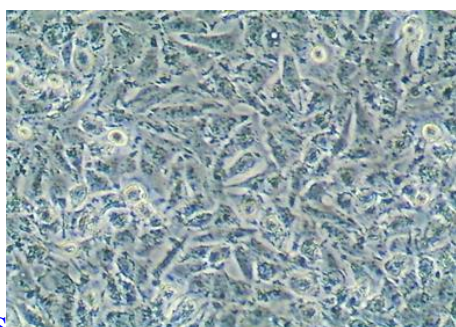


Figure (3): Dose-response curve of IC₅₀ for compound N4c at 72 hours.



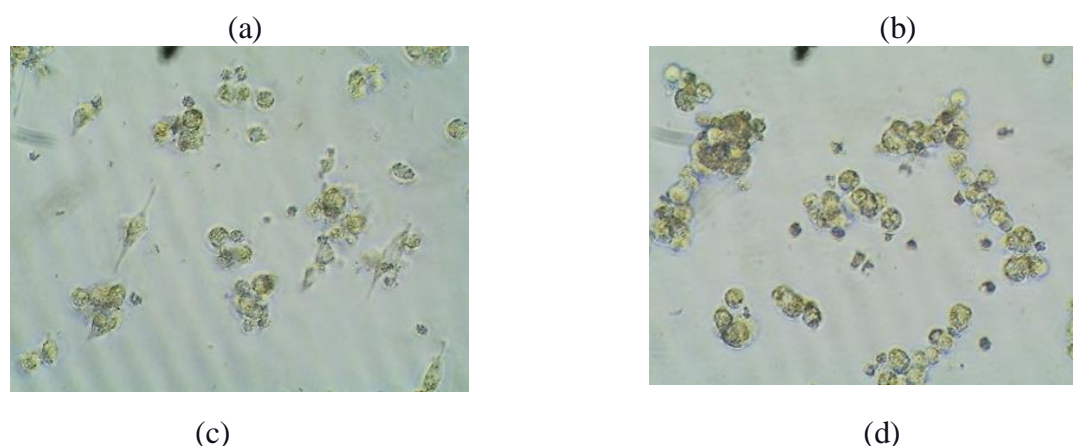


Figure (4): Morphological changes of A549 cell line after treatment with synthesized compounds at 48 hours under the microscope. a: control, b: N4a, c: N4b, d: N4c.

Conclusion

A new series of 1,3-diazetidone-2-one derivatives were successfully anticipated. *In-Silico* evaluation, including ADME studies, predicted that all of the compounds were passively and highly absorbed from the GIT. Furthermore, all of the newly anticipated compounds fulfilled the Lipinski “rule of five.” The molecular docking studies were conducted on the novel final compounds (N4a-c), which were the interaction of the ligands with EGFR proteins, and showed magnificent results in comparison to the reference drug (erlotinib). Successfully synthesized all of the intermediates (N1, N2, N3a-c) and the final compounds (N4a-c). The synthesized compounds were characterized using

melting point, and FT-IR spectroscopy, and confirmed using $^1\text{H-NMR}$ spectra and $^{13}\text{CNMR}$. The synthesized compounds were tested for their anticancer efficacy against the A549 lung cancer cell line. All of the produced compounds have impressive anti-proliferative activity except compound (N4c) has an IC_{50} of $12.77\ \mu\text{M}$, which is greater than erlotinib's IC_{50} of $11.5\ \mu\text{M}$ after 72 hours. The cytotoxicity investigation and molecular docking study on the novel compounds

(N4a-c) showed a very strong association.

Conflict of interest

Concerning this investigation, the authors have no conflicts of interest.

References

- 1- Dagogo-Jack I, Shaw AT. Tumour heterogeneity and resistance to cancer therapies. *Nat Rev Clin Oncol* 2018;15(2):81–94.
- 2- Hainaut P, Plymoth A. Cancer as a metabolic disease. *Curr Opin Oncol* 2012;24(1):56–7.
- 3- Hornberg JJ, Bruggeman FJ, Westerhoff H V., Lankelma J. Cancer: A Systems Biology disease. *BioSystems* 2006;83(2-3 SPEC. ISS.):81–90.
- 4- Zugazagoitia J, Guedes C, Ponce S, Ferrer I, Molina-Pinelo S, Paz-Ares L. Current Challenges in Cancer Treatment. *Clin Ther* 2016;38(7):1551–66. Available from: <http://dx.doi.org/10.1016/j.clinthera.2016.03.026>
- 5- Lemjabbar-Alaoui H, Hassan OUI, Yang YW, Buchanan P. Lung cancer: Biology and treatment options.



- Biochim Biophys Acta - Rev Cancer 2015;1856(2):189–210.
- 6- Hurley LH. DNA and its associated processes as targets for cancer therapy. Nat Rev Cancer 2002;2(3):188–200. Available from: <https://www.nature.com/articles/nrc749>
- 7- Rahim MA, Jan N, Khan S, Shah H, Madni A, Khan A, et al. Recent advancements in stimuli responsive drug delivery platforms for active and passive cancer targeting. Cancers (Basel) 2021;13(4):1–52.
- 8- Yewale C, Baradia D, Vhora I, Patil S, Misra A. Biomaterials Epidermal growth factor receptor targeting in cancer: A review of trends and strategies. Biomaterials 2013; Available from: <http://dx.doi.org/10.1016/j.biomaterials.2013.07.100>
- 9- Cho H soo, Mason K, Ramyar KX, Stanley AM. Structure of the extracellular region of HER2 alone and in complex with the Herceptin Fab. 2003;421(February).
- 10- Abdelgalil AA, Al-Kahtani HM, Al-Jenoobi FI. Erlotinib. Profiles Drug Subst Excip Relat Methodol 2020 ;45:93–117. Available from: <https://pubmed.ncbi.nlm.nih.gov/32164971/>
- 11- Borik RM, Fawzy NM, Abu-bakr SM, Aly MS. Docking Studies of Novel Heterocyclic Derivatives Obtained via Reactions Involving Curcumin. 2018;1–18.
- 12- The Importance of Heterocyclic Compounds in Anti-Cancer Drug Design - Drug Discovery World (DDW). Available from: <https://www.ddw-online.com/the-importance-of-heterocyclic-compounds-in-anti-cancer-drug-design-1106-201708/>
- 13- Suć Sajko J, Jerić I. Synthesis of Nβ-Substituted 1,2-Diazetidines by the Ugi Reaction Comprising Chiral α-Hydrazino Acids. J Org Chem 2022;87(11):7076–84.
- 14- Mahdi MF, Naser NH, Hammud NH. Synthesis and Preliminary Pharmacological Evaluation of New Naproxen Analogues Having 1, 2, 4-Triazole-3-Thiol. Int J Pharm Pharm Sci 2017;9(7):66.
- 15- Ammar YA, Khalifa MM, Eisa SI, Ismail MMF. New Naproxen Analogs: Synthesis, Docking and Anti-Inflammatory Evaluation. Polycycl Aromat Compd 2022;42(6):3586–605. Available from: <https://doi.org/10.1080/10406638.2020.1871037>
- 16- Mahdi MF, Al-smaism RF, Mahmood AI. Synthesis , Characterization of Some New 2-Azetidinone Derivatives. 2015;15(2).
- 17- Shi Y, Tang B, Yu PW, Tang B, Hao YX, Lei X, et al. Autophagy protects against oxaliplatin-induced cell death via ER stress and ROS in Caco-2 cells. PLoS One 2012; 7(11). Available from: <https://pubmed.ncbi.nlm.nih.gov/23226467/>
- 18- Kaplan A, Akalin Ciftci G, Kutlu HM. The apoptotic and genomic studies on A549 cell line induced by silver nitrate. Tumor Biol 2017;39(4).
- 19- Abdul-Majeed SZ, Mahdi MF, Al-Mugdadi SFH. Pharmacological Evaluation of New 4, 5-dihydro-1H-Pyrazole-1-yl acetate Derivatives as Anti-inflammatory Agents. Int J Drug Deliv Technol 2022;12(4):1733–41.
- 20- Amer M, Mahdi MF, Khan AK, Raauf AMR. Design, Molecular Docking, Synthesis, Preliminary In Silico ADME Studies, and Anti-inflammatory Evaluation of New Oxazole Derivatives. J Pharm Negat Results 2022;13(7):217–28.



- 21- Bickerton GR, Paolini G V., Besnard J, Muresan S, Hopkins AL. Quantifying the chemical beauty of drugs. Nat Chem 2012;4(2):90–8.
- 22- Hassanzadeh F, Jafari E, Zarabi M, Khodarahmi G, Vaseghi G. Synthesis, cytotoxic evaluation, and molecular docking studies of some new 1, 3, 4-oxadiazole-based compounds. Res Pharm Sci 2020;15(5):454–62.

